ELSEVIER

Journal of Orthopaedic Research 21 (2003) 1098–1106

Journal of Orthopaedic Research

www.elsevier.com/locate/orthres

Subject-specific finite element analysis of the human medial collateral ligament during valgus knee loading

John C. Gardiner [1], Jeffrey A. Weiss *

Department of Bioengineering, University of Utah, 50 S Central Campus Drive, Rm. 2480, Salt Lake City, UT 84112, USA

Received 1 January 2002; accepted 14 April 2003

Abstract

The objectives of this study were (1) to develop subject-specific experimental and finite element (FE) techniques to study the three-dimensional stress–strain behavior of ligaments, with application to the human medial collateral ligament (MCL), and (2) to determine the importance of subject-specific material properties and initial (in situ) strain distribution for prediction of the strain distribution in the MCL under valgus loading. Eight male knees were subjected to varus–valgus loading at flexion angles of 0°, 30°, and 60°. Three-dimensional joint kinematics and MCL strains were recorded during kinematic testing. Following testing, the MCL of each knee was removed to allow measurement of the in situ strain distribution and to perform material testing. A FE model of the femur–MCL–tibia complex was constructed for each knee to simulate valgus loading at each flexion angle, using subject-specific bone and ligament geometry, material properties, and joint kinematics. A transversely isotropic hyperelastic material model was used to represent the MCL. The MCL in situ strain distribution at full extension was used to apply in situ strain to each MCL FE model. FE predicted MCL strains during valgus loading were compared to experimental measurements using regression analysis. The subject-specific FE predictions of strain correlated reasonably well with experimentally measured MCL strains ($R^2 = 0.83$, 0.72, and 0.66 at 0°, 30°, and 60°, respectively). Despite large inter-subject variation in MCL material properties, MCL strain distributions predicted by individual FE models that used average MCL material properties were strongly correlated with subject-specific FE strain predictions ($R^2 = 0.99$ at all flexion angles). However, predictions by FE models that used average in situ strain distributions yielded relatively poor correlations with subject-specific FE predictions ($R^2 = 0.44$, 0.35, and 0.33 at flexion angles of 0°, 30°, and 60°, respectively). The strain distribution within the MCL was nonuniform and changed with flexion angle. The highest MCL strains occurred at full extension in the posterior region of the MCL proximal to the joint line during valgus loading, suggesting this region may be most vulnerable to injury under these loading conditions. This work demonstrates that subject-specific FE models can predict the complex, nonuniform strain fields that occur in ligaments due to external loading of the joint.

Keywords: Finite element; Ligament; Subject-specific modeling; Joint mechanics; MCL

Introduction

Despite the many investigations of ligament function, the exact mechanical role of specific ligaments in maintaining joint stability, the cause and effect of injuries, and the efficacy of various reconstructive procedures remain unclear or unknown. This is partially due to inherent limitations of experimental studies such as their high cost, low sensitivity, and the difficulties associated with accurate measurement of quantities such as strain and especially stress. The use of computational methods for the study of joint mechanics can elucidate ligament function and yield information that is difficult or impossible to obtain experimentally [2,3,9,16,17]. In particular, the finite element (FE) method offers the ability to predict spatial and temporal variations in stress, strain, and contact area/forces. The FE method also provides a standardized framework for parameter studies, such as evaluation of multiple clinical treatments, that can reduce both the cost and time of such studies. Subject-specific FE modeling of ligament stress–strain behavior can potentially accommodate the large inter-subject variability and eliminate noise in measurements due to random and systematic errors that can limit the sensitivity of experimental and clinical investigations. However, the exact subject-specific model inputs that

* Corresponding author. Tel.: +1-801-587-7833; fax: +1-801-585-5361.

E-mail address: jeff.weiss@utah.edu (J.A. Weiss).

[1] Present address: MacInnis Engineering Associates, Lake Forest, CA, USA.

0736-0266/$ - see front matter © 2003 Orthopaedic Research Society. Published by Elsevier Ltd. All rights reserved.
doi:10.1016/S0736-0266(03)00113-X

are necessary to obtain faithful predictions of ligament stress–strain behavior are unknown.

The vast majority of studies that have employed computational methods to study ligaments have used a one-dimensional representation of ligament geometry [3,12,33,46]. This entails using either single or multiple line elements [46], while allowing load transfer to bones at single or multiple points [5]. A one-dimensional representation requires only a few parameters to control load–elongation behavior, and overall in situ tension can be specified with a single scalar value. This approach has proved useful for predicting joint kinematics under the application of external loads (e.g., [23]), but it possesses several significant shortcomings: (1) nonuniform, 3D stresses and strains cannot be predicted, and (2) multiple sets of parameters and initial tensions routinely produce nearly identical predictions of joint kinematics. Ligaments are subjected to highly nonuniform deformations in vivo that result from a combination of tension, shear, bending, and compression [11,29], and the regional contribution of a ligament to joint stability changes with joint orientation [1,4,10,18,19,47]. A three-dimensional FE modeling approach is required to capture these characteristics.

Three-dimensional FE modeling of ligament stress–strain behavior is complicated by highly anisotropic, nonlinear material behavior and large deformations. To date, three-dimensional FE models of ligaments have incorporated greatly simplified representations of in situ strain (defined herein as the strain measured from a stress-free reference configuration) and have used average material properties and geometry [17,45], likely limiting their ability to predict subject-specific behavior. These limitations may be circumvented by incorporating subject-specific material properties, ligament and bony geometry, and in situ strain distributions. In addition to providing a basic science understanding of ligament mechanics and a framework for studying tissue-level deformations, subject-specific modeling techniques can be used for education and patient-specific surgical planning. Unfortunately, quantities such as ligament in situ strain distribution and material properties are time-consuming and difficult to measure in an experimental setting and nearly impossible to measure in a clinical setting. Model construction could be greatly simplified if average values could be used to represent these input quantities. However, the effects of average versus subject-specific model inputs on FE predictions of ligament mechanical behavior are unknown.

The objectives of this study were to develop subject-specific experimental and FE techniques to study the three-dimensional stress–strain behavior of ligaments, with application to the human medial collateral ligament (MCL), and to determine the importance of subject-specific material properties and in situ strain distribution for the prediction of the strain distribution in the MCL under valgus loading. The femur–MCL–tibia complex of the human knee was chosen for study because of the high incidence of MCL injuries [31] and the clinical importance of interactions between the MCL and the anterior cruciate ligament in restraining valgus rotations and anterior–posterior translations [13,37]. Further, the extra-articular location of the MCL simplifies experimental strain measurement and geometry extraction using medical imaging techniques. Strain distributions in the human MCL under valgus knee loading were measured experimentally and predicted using subject-specific FE models at three different knee flexion angles. Numerical experiments were performed to assess whether subject-specific FE models could predict experimentally measured MCL strain values, and to determine whether FE predictions would be affected by the use of average material properties or in situ strain distributions rather than subject-specific values.

Methods

Eight male knees (donor age = 50 ± 7 years, range 37–61) were subjected to a detailed experimental and computational protocol to study the stress–strain behavior of the human MCL during joint loading (Fig. 1). Briefly, each knee was subjected to valgus loading at flexion angles of 0°, 30°, and 60°. Joint kinematics and MCL strain were quantified during all tests. Following kinematic testing, the MCL was dissected free from the joint to allow measurement of in situ strain and to perform material tests on isolated MCL samples. FE models were created for each knee and validated on a subject-specific basis. Each model was constructed from experimental measurements of geometry, material properties, and kinematics and each model was validated by comparisons of experimental and FE predicted MCL strain during valgus loading.

Specimen preparation

The knees were allowed to thaw at room temperature for 12 h prior to dissection. All skin, muscle, and other periarticular soft tissue surrounding the knee joint were removed, including the patella and patellar tendon (Fig. 2). At the time of dissection, no signs of arthritis or previous soft tissue injury were found in any of the knees. The femur and tibia/fibula were secured in mounting tubes using a low-melt alloy. The mounting blocks for an instrumented spatial linkage (ISL, Endura-Tec, Eden Prairie, MN) were secured to the femur and tibia.

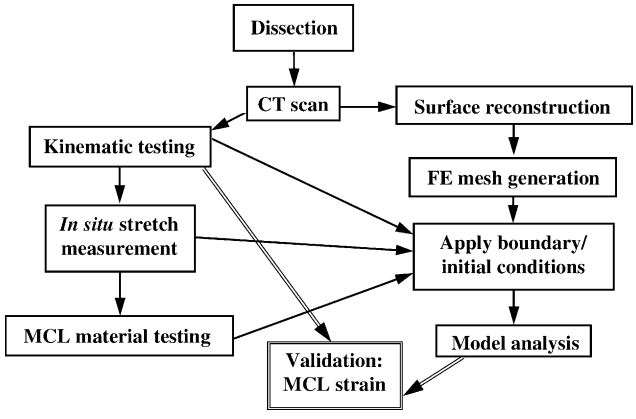

Fig. 1. Flow chart of combined experimental/computational protocol utilized for study of MCL mechanics during valgus loading.

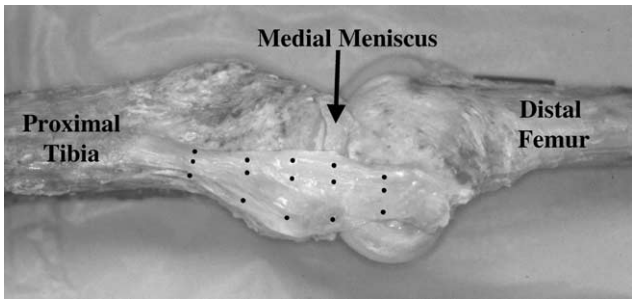

Fig. 2. Photograph of human knee (right) prepared for kinematic testing. All periarticular soft tissue has been removed and black markers have been attached to the MCL surface for regional strain measurement.

These blocks allowed spatial registration of the experimental and computational coordinate systems [7], while the ISL allowed continuous monitoring of joint kinematics during testing. The tissue was kept moist with 0.9% buffered saline applied via misting spray at three-minute intervals during all dissection and testing.

Volumetric CT scan acquisition

After dissection, a volumetric CT image dataset was obtained with the knee at zero degrees of flexion (Somatom Plus4; Siemens, Munich, Germany). An average of 225 slices were collected (12 bit resolution, 512×512 image matrix, FOV = 140 mm, slice thickness = 1.0 mm, on-center distance = 1.0 mm).

Kinematic testing

Each knee was mounted in a custom kinematic fixture on a servohydraulic testing machine (MTS, Eden Prairie, MN). Tibial axial rotation, medial-lateral translation, and joint distraction were unconstrained, while the anterior–posterior (A–P) tibial translation was constrained in a neutral position. A–P neutral position was defined as the midpoint between displacement limits from the tenth cycle of an A–P test between limits of ±5 N load applied to the tibia with the same fixtures. Embedded coordinate systems were established for the femur and tibia as defined by the Grood–Suntay convention [14] by digitizing anatomical points with the ISL via the method of Kirstukas et al. [20,21]. Kinematic testing was performed at fixed flexion angles of 0°, 30° and 60°, as determined from the Grood–Suntay representation of flexion angle [14]. Ten cycles of varus–valgus (V–V) rotation were applied at 1° per second to limits of ±10 N m torque at each flexion angle. V–V torque and rotation were recorded (accuracy of ±0.2 N m and ±0.1°, respectively) and data from the loading phase of the tenth valgus cycle were used for data analysis and modeling. The ISL provided continuous recording of rigid body motion (accuracy ±0.2° and ±0.2 mm for rotations and translations, respectively [21]).

Strain was measured on the MCL surface during all kinematic testing using a three-dimensional marker tracking system (Peak Performance Technologies, Englewood, CO). Prior to testing, 1.4 mm diameter markers were adhered to the MCL surface using cyanoacrylate. The markers formed a 3×5 grid and followed the local fiber direction between the MCL insertions, yielding 12 gauge lengths (15–20 mm) for measurement of fiber strain (Fig. 2). The marker tracking system was calibrated over a 350 cm^3 volume using the direct linear transformation method [38], allowing the 3D coordinates of the markers to be tracked to within ±0.1 mm during all testing [10]. The distance between marker pairs was computed from the three-dimensional coordinates, yielding the current length l.

In situ strain measurement

Following kinematic testing, the MCL in situ strain distribution was determined [10]. Briefly, the MCL was dissected free from its femoral, tibial, and meniscal attachments. The isolated MCL was placed on a saline covered glass plate and allowed to assume its stress-free configuration. The marker tracking system was used to determine the gauge lengths in the stress-free reference state (l_0) [47]. These data were combined with the gauge length measurements during kinematic testing (l) to calculate fiber-direction tensile strain between marker pairs as $\varepsilon = (l - l_0)/l_0$.

MCL material testing and constitutive modeling

Uniaxial tensile test specimens were harvested from the MCL parallel and transverse to the collagen fiber direction with hardened steel dogbone-shaped punches using an established protocol [34]. Cross-sectional area of the tensile test specimens was measured using digital calipers, assuming a rectangular cross-sectional area. The assumption of a rectangular cross-section was justified based on the geometry of the specimens obtained with the hardened steel punch. The stress–strain relationship was determined for longitudinal and transverse samples from the load–time (accuracy ±0.1 N) and strain–time (noncontact optical measurements, accuracy ±0.1%) data and the specimen cross-sectional area.

The MCL was represented as transversely isotropic hyperelastic with the following strain energy W [42]:

$$W = F_1(\tilde{I}_1) + F_2(\tilde{\lambda}) + \frac{K}{2}(\ln(J))^2. \tag{1}$$

Here $\tilde{I}_1$ is the first deviatoric invariant, $\tilde{\lambda}$ is the deviatoric part of the stretch ratio along the local fiber direction, and J is the determinant of the deformation gradient, $\boldsymbol{F}$. The three terms represent the contribution from the matrix, the collagen fibers, and the tissue volumetric response. The matrix strain energy F_1 was chosen so that $\partial F_1/\partial \tilde{I}_1 = C_1$, yielding the neo-Hookean constitutive model [34]. The derivatives of the fiber strain energy function F_2 were defined as a function of the fiber stretch:

$$\begin{aligned}
&\tilde{\lambda}\frac{\partial F_2}{\partial \lambda} = 0, \quad \tilde{\lambda} \leqslant 1;\\
&\tilde{\lambda}\frac{\partial F_2}{\partial \lambda} = C_3[\exp(C_4(\tilde{\lambda} - 1)) - 1], \quad 1 < \tilde{\lambda} < \lambda^*;\\
&\tilde{\lambda}\frac{\partial F_2}{\partial \lambda} = C_5\tilde{\lambda} + C_6, \quad \tilde{\lambda} \geqslant \lambda^*.
\end{aligned} \tag{2}$$

C_3 scales the exponential stress, C_4 specifies the rate of collagen uncrimping, C_5 is the modulus of straightened collagen fibers, and λ^* is the stretch at which the collagen is straightened. Material parameters were determined via a nonlinear regression procedure [34]. The bulk modulus K controlled the entire volumetric response of the material. Due to a lack of experimental data describing ligament bulk behavior, the bulk modulus was specified to be two orders of magnitude greater than C_1, yielding nearly incompressible material behavior.

Finite element models

The surface geometries of the femur, MCL, and tibia of each knee were obtained from the CT data. Polygonal surfaces of the femur and tibia were extracted using marching cubes [24] with decimation [36] (Fig. 3A). Cross-sectional contours of the superficial MCL were digitized from each CT slice and a polygonal surface of the MCL was generated from the contours [6]. Surfaces were imported into a FE preprocessing program (TrueGrid, XYZ Scientific, Livermore, CA) and hexahedral FE meshes were constructed for each structure (Fig. 3B). Models consisted of approximately 25,000 elements.

Boundary conditions

The experimentally measured 3D kinematics were used to prescribe motions of the FE model. The femur and tibia were represented as rigid bodies. This reduced the computational expense of the model by allowing bone motions to be represented by three translations and three rotations. The coordinates of the ISL mounting blocks in the CT-defined coordinate system allowed correlation of kinematic measurements with geometric data [7]. The entire FE model was translated and rotated so that the global coordinate system was aligned with the coordinate system of the tibial ISL block. Rigid body motion was described by incremental translations and rotations referenced to coordinate systems at the ISL mounting blocks [25,26]. Incremental rotations were extracted from the transformation matrix using the method of Simo and Vu-Quoc [39].

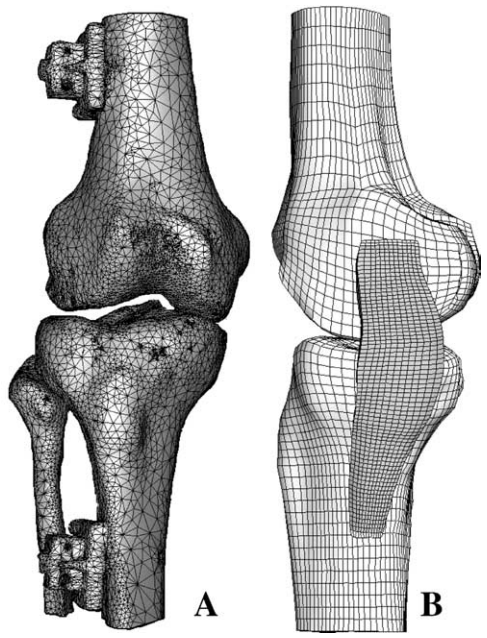

Fig. 3. (A) Polygonal surfaces representing the femur and tibia of one of the eight knees as extracted from volumetric CT data. (B) Hexahedral finite element meshes of femur, MCL, and tibia.

The MCL FE mesh was attached to the femur and tibia by specifying the final row of elements at the proximal and distal ends of the ligament to be part of the same rigid material as the corresponding bone. To accurately model the direct insertion site characteristic of the femoral attachment of the MCL, the mesh was refined allowing the final 3–5 mm of the MCL to curve and meet the bone at approximately a 90° angle. There was no representation in the model of the attachment of the superficial MCL to the deeper fibers of the MCL or to the medial meniscus. Contact and load transfer between the MCL and bones was accommodated using the penalty method [44].

The in situ strains that were measured experimentally during passive flexion were applied to the FE models [8,43]. Failure to include this in situ strain distribution can lead to gross underestimation of the actual stress and strain. Three distinct configurations were proposed: the stress-free state (0), the in situ strain state (R), and the current or deformed state (r). This allowed the total deformation gradient, $\boldsymbol{F}_{r0}$ to be expressed as a multiplicative decomposition of the deformation gradients between the three states:

$$\boldsymbol{F}_{r0} = \boldsymbol{F}_{rR}\boldsymbol{F}_{R0}. \tag{3}$$

Here, $\boldsymbol{F}_{R0}$ represents the deformation gradient due to the in situ strains and $\boldsymbol{F}_{rR}$ is the deformation gradient that results from other applied loads, as determined from the search for equilibrium by the FE code. As an initial estimate, $\boldsymbol{F}_{R0}$ was assumed to be a uniaxial stretch,

$$[F_{R0}] = \begin{bmatrix} \lambda & 0 & 0 \\ 0 & 1 & 0 \\ 0 & 0 & 1 \end{bmatrix}, \tag{4}$$

where λ is the local fiber-direction stretch. The experimental in situ fiber strain values between discrete points on the MCL were interpolated over the FE mesh to apply a continuous range of in situ strain over the entire MCL mesh. An iterative update algorithm was used to determine the final values for the components of $\boldsymbol{F}_{R0}$ by ensuring that the experimentally measured in situ strain value λ was satisfied exactly at each integration point in the mesh [8].

Finite element solution procedure

The implicitly integrated FE code NIKE3D was used for all analyses [25]. The FE analysis was performed in two phases. During the first phase, the in situ strains were applied while the femur was moved from the CT scanning position to the current passive flexion position (0°, 30°, or 60°). During the second phase, experimental knee kinematics corresponding to valgus rotation were applied. An automatic timestepping strategy was employed, with iterations based on a quasi-Newton method [28] and convergence based on the L_2 displacement norm [25,28]. The FE postprocessing software GRIZ (Lawrence Livermore National Laboratory, Livermore, CA) was used to visualize the results. FE predictions for fiber strain were obtained from locations corresponding to the experimental discrete measurement regions. The FE models were also used to predict the magnitude and direction of ligament forces at the insertion sites as well as the resultant force due to contact as the MCL wraps around the tibia.

Parameter studies

The necessity of using subject-specific modeling techniques was assessed for two quantities that would be difficult to quantify on an individual basis for in vivo studies: material properties and in situ strain distribution. All eight knee models were reanalyzed using subject-specific in situ strains and average MCL material properties and then again using average MCL in situ strain distributions and subject-specific material properties.

Statistical analysis

Regression analyses were used to evaluate the ability of the subject-specific FE models to predict experimentally measured values of MCL strain. Coefficients of determination (R^2), regression lines, 95% confidence intervals, and p-values were calculated for each of the 12 measurement regions. To simplify presentation, a combined analysis was also performed in which all measurement regions were combined in a single regression analysis at each flexion angle. Scatter plots of the combined datasets showing subject-specific FE model strains versus experimentally measured strains were generated for flexion angles of 0°, 30°, and 60°. Data from the most posterior-proximal region were not included in the combined regression analyses because of ligament buckling during experimental measurements. Regression analyses were also used to compare subject-specific FE model predictions of strain with strain predictions from the FE models that used average material properties and in situ strain distributions.

Results

MCL strain was nonuniform at all flexion angles for passive flexion as well as with valgus rotation [10]. During passive flexion, fiber strain varied between 1% and 5% depending on the region and flexion angle. At full extension, the largest strains occurred in the posterior fibers while the smallest strains were in the anterior fibers. With increasing flexion angle, strain generally decreased in the posterior and central MCL regions while strain along the anterior border remained relatively constant. Valgus rotation caused an increase in MCL fiber strain compared to the unloaded configuration for all regions and flexion angles. The regional differences and trends were similar to those observed for passive flexion. Complete results of the experimental strain measurements can be found in our previous work [10].

Experimental measurements of MCL tensile material behavior confirmed the highly anisotropic nature of this tissue. Specimens tested along the fiber direction exhibited the upwardly concave stress–strain behavior characteristic of collagenous tissues. The transverse

Table 1
Material coefficients for the transversely isotropic, hyperelastic constitutive model determined via nonlinear curve-fitting of experimental stress–strain data

Specimen	C_1 (MPa)	λ^*	C_3 (MPa)	C_4 (no units)	C_5 (MPa)
1	1.50	1.055	0.493	47.9	356.8
2	1.29	1.080	0.120	48.3	327.4
3	1.28	1.100	0.352	31.1	352.4
4	1.09	1.055	0.488	46.2	363.5
5	1.13	1.045	0.539	66.8	823.7
6	1.79	1.060	0.854	38.0	401.6
7	1.41	1.060	1.303	40.6	462.3
8	2.05	1.050	0.387	65.2	649.1
Mean ± std	1.44 ± 0.33	1.062 ± 0.018	0.57 ± 0.36	48.0 ± 12.5	467.1 ± 177.4

specimens had a nearly linear stress–strain relationship and were approximately two orders of magnitude less stiff than the specimens tested along the fiber direction. The material coefficients obtained by curve-fitting the stress–strain data to the transversely isotropic material model [34] indicate the variability in tangent modulus (C_5) and fiber uncrimping length (λ^*) between specimens (Table 1).

Predictions of strain from subject-specific FE models were correlated with experimentally measured MCL strain during valgus loading, although the degree of correlation depended on the particular region and flexion angle (Figs. 4 and 5). The means of the R^2 values for the 12 regions at each flexion angle were 0.73 ± 0.14, 0.75 ± 0.15, and 0.55 ± 0.32 for flexion angles of 0°, 30° and 60°, respectively. There were not any apparent trends in the variation of R^2 values with region, with the exception that all R^2 values were very low ($R^2 \leqslant 0.1$) in the three proximal regions at 60° flexion. The regression analyses that combined all measurement regions at each flexion angle indicated that subject-specific FE predictions of strain were correlated with the experimental measurements at all three flexion angles ($p < 0.001$ at all flexion angles; $R^2 = 0.83$, 0.72, and 0.66 at 0°, 30°, and 60°, respectively). The R^2 values indicate a decreasing correlation between the models and experiments with increasing flexion angle, while the 95% confidence intervals demonstrated that the true best fit line fell within a very small area around the fitted lines (Fig. 5).

Even during passive flexion, tensile forces exist in the MCL due to the in situ strains. The FE models predicted forces that varied with flexion angle (mean ± standard deviation) at the insertion sites of both the tibia (25.8 ± 10.6, 10.8 ± 6.9, and 22.6 ± 22.1 N at angles of 0°, 30°, and 60°, respectively) and femur (24.4 ± 9.7, 10.5 ± 6.7, and 22.7 ± 21.7 N at angles of 0°, 30°, and 60°, respectively). After application of 10 N m valgus torque, the insertion site forces increased at both the tibia (111.7 ± 49.0, 82.5 ± 51.5, and 96.5 ± 91.0 N at 0°, 30°, and 60°, respectively) and femur (107.4 ± 47.0, 78.5 ± 48.6, and 95.6 ± 83.2 N at 0°, 30°, and 60°, respectively). Valgus loading was accompanied by contact forces at the midsubstance location where the MCL wraps around the tibia (20.8 ± 11.8, 15.8 ± 11.5, and 15.3 ± 24.8 N at 0°, 30°, and 60°, respectively).

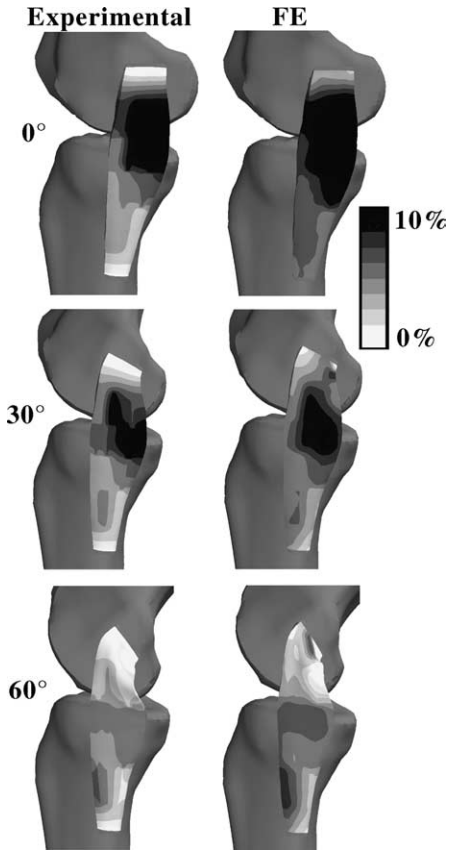

Fig. 4. MCL fiber direction strain after application of 10 N m valgus torque at flexion angles of 0°, 30°, and 60° for experimental measurements (left column) and subject-specific FE models (right column) for a representative knee. The discrete experimental values have been interpolated onto the FE mesh to generate a continuous spatial representation of results.

The use of average material properties instead of subject-specific properties had very little effect on FE predictions of strain (Fig. 6, $R^2 = 0.99$, $p < 0.001$ at all flexion angles). In contrast, use of an average in situ strain distribution resulted in relatively poor predictions

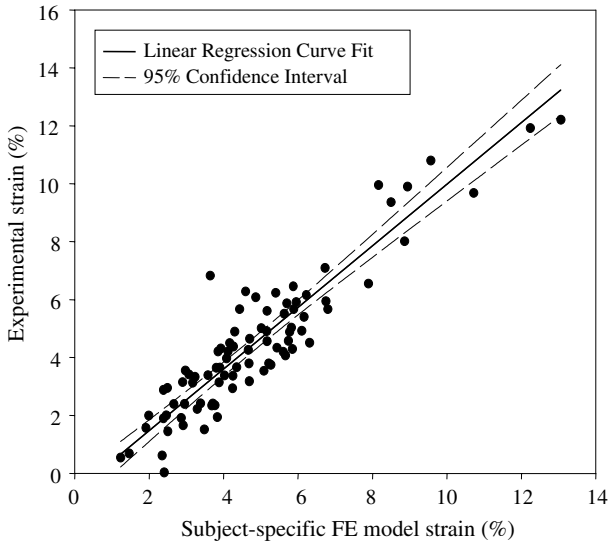

Fig. 5. Scatter plots of MCL strain (%) for subject-specific FE models vs. experimental measurements during peak valgus loading for all eight specimens at a flexion angle of 0°.

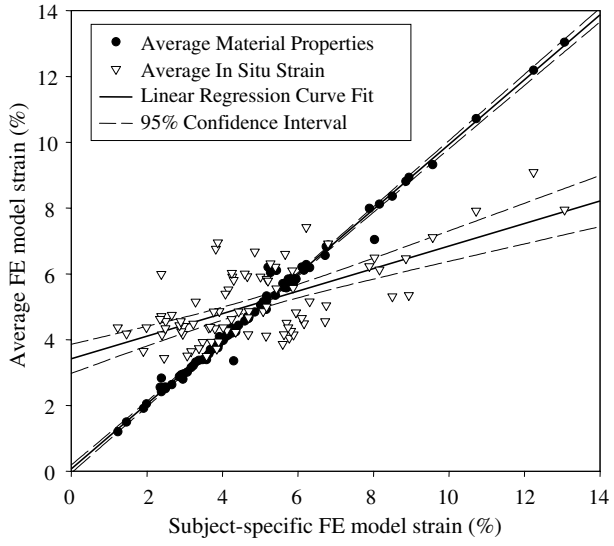

Fig. 6. Scatter plots of MCL strain (%) from subject-specific FE models vs. models featuring average material properties (●) and average initial tension (▽) for all eight specimens at a flexion angle of 0°.

of subject-specific strain during valgus loading ($R^2 = 0.44$, 0.35, and 0.33 at flexion angles of 0°, 30°, and 60°, respectively).

Discussion

The objectives of this study were to develop subject-specific experimental and FE techniques to study the three-dimensional stress–strain behavior of ligaments, with application to the human MCL, and to determine the importance of subject-specific material properties and in situ strain distribution for the prediction of the strain distribution in the MCL under valgus loading. FE models with subject-specific geometry, material properties, and boundary conditions (in situ strain and kinematics) resulted in generally good predictions of experimental MCL strains (Figs. 4 and 5). Despite large inter-subject variation in MCL material properties, the use of average material properties did not have a significant effect on subject-specific FE model predictions of regional strain (Fig. 6). However, FE models with average in situ strain values and subject-specific material properties, geometry, and kinematics did not provide accurate predictions of subject-specific FE predictions (Fig. 6).

The experimental and FE-predicted MCL strains reported in the current study are supported by the data of previous experimental, computational, and clinical studies. Hull et al. [18] reported similar trends for strain distribution in the anterior fibers of the MCL. Strain increased with valgus loading and regional differences in strain with changes in flexion angle were consistent with the current study. However, the magnitudes of strain reported in their study were in general lower than those in the present study. As an extreme example, we measured a strain of $7.9 \pm 3.8\%$ for the region labeled posterior–superior in the Hull et al. study [10], while that study reported a strain of 3.5 ± 3.1. Nevertheless, the percent differences in strain between regions are comparable. The differences in strain magnitude can be attributed to differences in the level of joint loading (± 10 N m varus–valgus torque presently versus ± 7 N m in the Hull study), strain measurement technique (optical versus liquid mercury strain gauge), and method for establishing the ligament reference length. Arms et al. [1] also reported changes in strain in the human MCL under valgus loading. In general their results are consistent with the presently reported results under application of valgus loading, although the manner of torque application and joint degrees of freedom used in their study were quite different from the present study. For instance, they reported an increase in strain in the anterior portion of the MCL with knee flexion under valgus loading. Direct comparison with our results is further complicated because a true zero-strain state was not established in their study.

It is interesting to note that the highest strains of approximately 10% occurred in the posterior proximal region of the MCL near the femoral insertion. This was under the relatively low level of 10 N m valgus loading at 0° flexion, suggesting this region may be most vulnerable to injury under similar loading conditions. Although prior experimental investigations have not quantified strain in this region, a FE knee model using a one-dimensional representation for discrete regions of the MCL also predicted the highest strains in this region [3].

Clinical injury patterns also confirm that the posterior proximal region of the MCL is the most common injury location [19,22]. Injuries in this area generally do not heal as well as those located distal to the joint line [35]. Strain may increase more slowly in this region at higher strain levels due to greater load sharing within the MCL as a result of increased axial rotation.

The subject-specific FE models provided the best predictions of experimental strain values at 0° and 30° flexion (overall $R^2 = 0.73 \pm 0.14$ and 0.75 ± 0.15, respectively), which corresponded to the flexion angle used for CT imaging and model construction. The less accurate predictions at 60° of flexion (overall $R^2 = 0.55 \pm 0.32$) are partly due to the increased complexity of the deformation with increasing flexion angle. The joint orientation used for geometry acquisition may not be as crucial if the structure of interest does not experience extreme deformations. Also, FE predictions at 30° and 60° required that flexion of the knee from 0° was first simulated. This likely introduced additional error in the predictions by emphasizing potential inaccuracy in the assumed constitutive behavior of the MCL.

Numerical experiments that examined the effects of average material properties and average in situ strain distributions provided insight into the importance of subject-specific model input parameters. The FE strain predictions were insensitive to the use of average material properties. This was demonstrated by a very strong correlation between FE predictions that utilized subject-specific material properties for each model versus model predictions using average properties (Fig. 6). In contrast, an average in situ strain distribution resulted in relatively poor predictions of subject-specific strain during valgus loading. The latter observation is unfortunate, as it suggests that subject- or patient-specific FE predictions may necessitate a means to measure the in situ strain distribution.

The three-dimensional, subject-specific modeling approach used in the current study offers several advantages over previous approaches for describing and predicting the load–elongation and stress–strain behavior of ligaments. Three-dimensional FE models allow shear, compression, and bending to be represented more accurately than is possible with discrete element ligament models. In addition, the subject-specific approach allows incorporation of individual material properties, geometry, and boundary conditions. Previous studies have used a single model based on the geometry of one specimen and assigned some assumed or average material properties and boundary conditions. The use of "average" models can in fact be useful for predicting general trends in mechanical behavior; however, it may not be possible to accurately predict stress and strain on a subject-specific basis with such an approach (Fig. 6). Although the present study did not examine the effects of an "average" geometry for subject-specific prediction of MCL strains using the FE method, this was primarily because it was unclear as to how an appropriate average geometry should be constructed. Further, of all necessary subject-specific inputs, geometry is arguably the easiest to generate since it can be obtained readily from medical image data. Although the current studies were based on cadaveric knees, the geometry extraction methods can be used to create patient-specific models from medical image data obtained in vivo. In contrast, in vivo measurements of ligament material properties and in situ strains would be extremely difficult.

The robustness and range of utility of subject-specific ligament FE models could be improved by using adaptive meshing strategies. The MCL is subjected to large deformations during joint motions and the extreme material distortion is challenging to model using the FE method. During simulated flexion, some finite elements became severely distorted as knee flexion proceeded beyond 60°, resulting in element inversion. This was especially problematic near the femoral insertion of the MCL. Remeshing or rezoning could potentially alleviate some of these problems [30]. With such an approach, the FE mesh could be "reset" periodically throughout an analysis to reduce element distortion and facilitate the accurate simulation of larger deformations.

Although the transversely isotropic hyperelastic material model [42] used in this study accurately describes longitudinal and transverse tensile behavior of the MCL [34], there are improvements that could be made to the material representation. The response of the strain energy function used in this study may be too stiff under shear loading as evidenced by large deformation simple shear loading of MCL samples [41]. This suggests that fiber–fiber interactions such as crosslinking may be responsible for the majority of the transverse material stiffness and that these crosslinks have a reduced shear resistance due to an initial transverse orientation. A new constitutive model that describes all three sets of material test data (longitudinal tension, transverse tension, finite simple shear) is under development. Further improvements in modeling accuracy could be achieved by including inhomogeneities in MCL material properties that likely occur throughout the ligament substance [32]. The method of material characterization used in this study prohibits quantifying material properties throughout the entire MCL because of the needed sample sizes, but histological [32] or optical [15] measurements could be utilized to estimate material properties on a regional basis. Improved data for material properties and geometry near the ligament insertions to bone would enhance the predictive capability of the models in those regions. This could be achieved by transitioning material properties and geometry to better simulate in vivo structure. Unfortunately, the variations in material properties near ligament insertions to bone occur over such a small distance that they are difficult to

quantify experimentally. Finally, incorporation of three-dimensional viscoelastic behavior could provide insight into injury mechanisms during sporting activities.

To simplify the FE model geometry, it was assumed that the superficial MCL interactions with the deep fibers of the MCL and the medial meniscus did not substantially influence the MCL strain distribution. In two of the knees in this series, varus–valgus rotation was determined both before and after the MCL attachment to the meniscus was sectioned. Sectioning did not change the amount of varus–valgus rotation under ±10 N m applied varus–valgus torque at any of the flexion angles. This is in agreement with the results of other studies [13,27,37,40]. However, we did not examine the strain distributions in the MCL after sectioning of the meniscal attachment. Thus it is possible that the absence of MCL interaction with the meniscus affected the ability of the FE models to predict the experimental strains. This would likely be most problematic at larger flexion angles as the posterior aspect of the MCL buckles, and may in fact explain the poorer correlations between experimental measurements and FE predictions at 60° of knee flexion. Future models could be improved by allowing force transfer through interactions of the superficial MCL with the medial meniscus or deep fibers of the MCL, but the CT image data used in this study did not allow easy visualization of the boundaries of these structures.

In summary, experimental and computational methods have been developed and validated for study of the three-dimensional deformation of the human MCL during passive flexion and valgus rotation of the knee. A subject-specific FE modeling technique was used to predict experimental strain measurements as well as insertion site and contact forces. Numerical techniques such as the current FE models are essential to accurately characterize the complex deformations that occur in soft tissue structures such as ligaments and to quantify the resultant nonuniform stress and strain fields on tissue and microstructural levels. The methodologies developed in this work can be readily adapted to the study of other ligamentous structures and joints. This should provide a solid foundation for further studies of ligament injury, healing, and patient-specific clinical treatment.

Acknowledgements

Financial support from the Whitaker Foundation and NIH #AR47369 is gratefully acknowledged.

References

[1] Arms S, Boyle J, Johnson R, Pope M. Strain measurement in the medial collateral ligament of the human knee: an autopsy study. J Biomech 1983;16:491–6.

[2] Atkinson TS, Haut RC, Altiero NJ. A poroelastic model that predicts some phenomological responses of ligaments and tendons. J Biomech Eng 1997;119:400–5.

[3] Bendjaballah MZ, Shirazi-Adl A, Zukor DJ. Finite element analysis of human knee joint in varus–valgus. Clin Biomech (Bristol, Avon) 1997;12:139–48.

[4] Berns GS, Hull ML, Patterson HA. Strain in the anteromedial bundle of the anterior cruciate ligament under combination loading. J Orthop Res 1992;10:167–76.

[5] Blankevoort L, Huiskes R. Ligament–bone interaction in a three-dimensional model of the knee. J Biomech Eng 1991;113:263–9.

[6] Boissonnat JD. Shape reconstruction from planar cross-sections. Comp Vision, Graphics Image Process 1988;44:1–29.

[7] Fischer KJ, Manson TT, Pfaeffle HJ, et al. A method for measuring joint kinematics designed for accurate registration of kinematic data to models constructed from CT data. J Biomech 2001;34:377–83.

[8] Gardiner JC, Maker BN, Weiss JA. An iterative update algorithm to enforce initial stretch in hyperelastic finite element models of soft tissue. Proc ASME Summer Bioengineering Conference 2001. p. 359–60.

[9] Gardiner JC, Weiss JA. Experimental testing and computational modeling to determine the stress–strain distribution in the human medial collateral ligament. Trans 44th Annual Orthopaedic Research Society 1998;23(2):1027.

[10] Gardiner JC, Weiss JA, Rosenberg TD. Strain in the human medial collateral ligament during valgus loading of the knee. Clin Orthop 2001;391:266–74.

[11] Giori NJ, Beaupre GS, Carter DR. Cellular shape and pressure may mediate mechanical control of tissue composition in tendons. J Orthop Res 1993;11:581–91.

[12] Grood ES, Hefzy MS. An analytical technique for modeling knee joint stiffness—Part I: Ligamentous forces. J Biomech Eng 1982;104:330–7.

[13] Grood ES, Noyes FR, Butler DL, Suntay WJ. Ligamentous and capsular restraints preventing straight medial and lateral laxity in intact human cadaver knees. J Bone Joint Surg (Am) 1981; 63:1257–69.

[14] Grood ES, Suntay WJ. A joint coordinate system for the clinical description of three-dimensional motions: application to the knee. J Biomech Eng 1983;105:136–44.

[15] Hansen KA, Weiss JA, Barton JK. Recruitment of tendon crimp with applied tensile strain. ASME J Biomech Eng 2002;124:72–7.

[16] Heegaard J, Leyvraz PF, Curnier A, et al. The biomechanics of the human patella during passive knee flexion. J Biomech 1995; 28:1265–79.

[17] Hirokawa S, Tsuruno R. Three-dimensional deformation and stress distribution in an analytical/computational model of the anterior cruciate ligament. J Biomech 2000;33:1069–77.

[18] Hull ML, Berns GS, Varma H, Patterson HA. Strain in the medial collateral ligament of the human knee under single and combined loads. J Biomech 1996;29:199–206.

[19] Kawada T, Abe T, Yamamoto K, et al. Analysis of strain distribution in the medial collateral ligament using a photoelastic coating method. Med Eng Phys 1999;21:279–91.

[20] Kirstukas SJ, Lewis JL, Erdman AG. 6R instrumented spatial linkages for anatomical joint motion measurement—Part 1: Design. J Biomech Eng 1992;114:92–100.

[21] Kirstukas SJ, Lewis JL, Erdman AG. 6R instrumented spatial linkages for anatomical joint motion measurement—Part 2: Calibration. J Biomech Eng 1992;114:101–10.

[22] Lee JI, Song IS, Jung YB, et al. Medial collateral ligament injuries of the knee: ultrasonographic findings. J Ultrasound Med 1996; 15:621–5.

[23] Li G, Kanamori A, Woo SL-Y. A validated three-dimensional computational model of a human knee joint. J Biomech Eng 1999;121:657–62.

[24] Lorensen WE, Cline HE. Marching cubes: a high resolution 3D surface construction algorithm. Comp Graph (Proc SIGGRAPH) 1987;4:163–9.
[25] Maker BN. NIKE3D: A nonlinear, implicit, three-dimensional finite element code for solid and structural mechanics. Lawrence Livermore Lab Tech Rept 1995; UCRL-MA-105268.
[26] Maker BN. Rigid bodies for metal forming analysis with NIKE3D. University of California, Lawrence Livermore Lab Rept 1995; UCRL-JC-119862 1–8.
[27] Markolf KL, Mensch JS, Amstutz HC. Stiffness and laxity of the knee—the contributions of the supporting structures. A quantitative in vitro study. J Bone Joint Surg (Am) 1976;58:583–94.
[28] Matthies H, Strang G. The solution of nonlinear finite element equations. Int J Numer Meth Eng 1979;14:1613–26.
[29] Matyas JR, Anton MG, Shrive NG, Frank CB. Stress governs tissue phenotype at the femoral insertion of the rabbit MCL. J Biomech 1995;28:147–57.
[30] Mei Z, Liu Y, Yang H. Research on a new remeshing method for the 3D FEM simulation of blade forging. J Mater Process Technol 1999;94:231–4.
[31] Miyasaka KC, Daniel DM, Stone ML, Hirshman P. The incidence of knee ligament injuries in the general population. Am J Knee Surg 1991;4:3–8.
[32] Mommersteeg TJ, Blankevoort L, Kooloos JG, et al. Nonuniform distribution of collagen density in human knee ligaments. J Orthop Res 1994;12:238–45.
[33] Mommersteeg TJ, Huiskes R, Blankevoort L, et al. A global verification study of quasi-static knee model with multi-bundle ligaments. J Biomech 1996;29:1659–64.
[34] Quapp KM, Weiss JA. Material characterization of human medial collateral ligament. J Biomech Eng 1998;120:757–63.
[35] Robins AJ, Newman AP, Burks RT. Postoperative return of motion in anterior cruciate ligament and medial collateral ligament injuries. The effect of medial collateral ligament rupture location. Am J Sports Med 1993;21:20–5.
[36] Schroeder WJ, Zarge J, Lorensen WE. Decimation of triangle meshes. Comp Graph (Proc SIGGRAPH) 1992;25.
[37] Seering WP, Piziali RL, Nagel DA, Schurman DJ. The function of the primary ligaments of the knee in varus–valgus and axial rotation. J Biomech 1980;13:785–94.
[38] Shapiro R. Direct linear transformation method for three-dimensional cinematography. Res Quart 1978;49:197–205.
[39] Simo JC, Vu-Quoc L. On the dynamics in space of rods undergoing large deformations—a geometrically exact approach. Comp Meth Appl Mech Eng 1988;66:125–61.
[40] Warren LF, Marshall JL, Girgis F. The prime static stabilizer of the medial side of the knee. J Bone Joint Surg (Am) 1974;56:665–74.
[41] Weiss JA, Gardiner JC, Bonifasi-Lista C. Ligament material behavior is nonlinear, viscoelastic and rate-independent under shear loading. J Biomech 2002;35:943–50.
[42] Weiss JA, Maker BN, Govindjee S. Finite element implementation of incompressible, transversely isotropic hyperelasticity. Comp Meth Appl Mech Eng 1996;135:107–28.
[43] Weiss JA, Maker BN, Schauer DA. Treatment of initial stress in hyperelastic finite element models of soft tissues. ASME Advances in Bioengineering 1995;BED-29:105–6.
[44] Weiss JA, Schauer DA, Gardiner JC. Modeling contact in biological joints using penalty and augmented Lagrangian methods. ASME Advances in Bioengineering 1996;BED-23:347–8.
[45] Wilson AN, Shrive NG, Frank CB. Verification of a three-dimensional ligament model. In: Middleton J, Jones ML, Pande GN, editors. Computer Methods in Biomechanics and Biomedical Engineering. New York: Gordon and Breach; 1996.
[46] Wismans J, Veldpaus F, Janssen J, et al. A three-dimensional mathematical model of the knee-joint. J Biomech 1980;13:677–85.
[47] Woo SL-Y, Weiss JA, Gomez MA, Hawkins DA. Measurement of changes in ligament tension with knee motion and skeletal maturation. J Biomech Eng 1990;112:46–51.